The 1st Joint International Conference on Multibody System Dynamics
May 25–27, 2010, Lappeenranta, Finland

Modeling a Coriolis Mass Flow Meter for Shape Optimization

W.B.J. Hakvoort [*], **J.P. Meijaard**[#], **R.G.K.M. Aarts**[#], **J.B. Jonker**[#], **J.M. Zwikker**[*]

[*] Demcon Advanced Mechatronics
Zutphenstraat 25, 7575 EJ Oldenzaal, The Netherlands
e-mail: wouter.hakvoort, rini.zwikker@demcon.nl
[#] Faculty of Engineering Technology - Mechanical Automation and Mechatronics
University of Twente.
P.O. Box 217, 7500 AE, Enschede, The Netherlands
e-mail: {j.p.meijaard, r.g.k.m.aarts, j.b.jonker}@utwente.nl

ABSTRACT

Modeling a Coriolis mass-flow meter for shape optimization is considered. The optimization should enhance the performance of the meter by improving several performance criteria like the measurement sensitivity. These performance criteria are improved by optimizing parameters that define the shape of the tube in the mass-flow meter. A dynamic model is used to obtain the performance criteria for a set of shape parameters. The tube is modeled using a flexible multibody approach, where an existing beam-element is modified to include the effect of the fluid flow. Besides the calculation of the performance criteria, the model is used to calculate the sensitivities of the performance criteria to the shape parameters, because those sensitivities are useful for the optimization. Results from modeling the performance criteria and the parameter sensitivities are shown for a U-shaped Coriolis mass-flow meter. Finally, some preliminary results from shape optimization are demonstrated.

Keywords: Flexible Multibody Dynamics, Fluid-Conveying Pipes, Modal Analysis, Sensitivity Analysis, Coriolis Mass-Flow Meter

1 INTRODUCTION

Coriolis mass flow meters measure the mass flow of a fluid from the vibration of a tube conveying that fluid. The tube is fixed at both ends and excited in one of its eigenmodes. A mass flow through the tube causes parts of the tube to vibrate out of phase resulting in a wave like motion. The motion of the tube is measured at two locations and the phase difference between the motion at those points is proportional to the mass flow. The phase difference per unit of flow is referred to as the measurement sensitivity of the mass flow meter. Measuring the mass flow from the Coriolis effect is advantageous, because the measurement is not affected by medium properties like density, viscosity and heat conductivity.

Several applications require the measurement of mass flows as little as 1 g/h, leading to a need for highly sensitive mass flow meters. Coriolis mass flow meters with small tubes are needed to measure such small flows, because the measurement sensitivity increases with the inverse of the size of the tube. However, scaling the tube dimensions does not increase the measurement sensitivity by the same factor the flow decreases and thus it is hard to measure small flows accurately. Many different tube shapes for Coriolis mass flow meters are claimed in patents and publications to maximize the measurement sensitivity, though the design of the tube shapes is mostly based on intuition. Improvement in terms of measurement sensitivity is expected from designing the tube shape using rigorous model-based optimization. Model-based optimization requires the formulation of appropriate performance criteria, the quantification of those performance criteria for a tube shape using a dynamic model and the application of a suitable optimization procedure to find the optimal tube shape. The focus of this paper is on modeling the dynamic properties for a given tube shape and on predicting the change of the dynamic properties with the tube shape. The relevant performance criteria and the optimization are outlined only briefly.

In Reference [8] it is shown that the measurement sensitivity of a Coriolis mass flow meter can be obtained from a dynamic model that describes the inertia and stiffness properties of the tube and the inertia properties

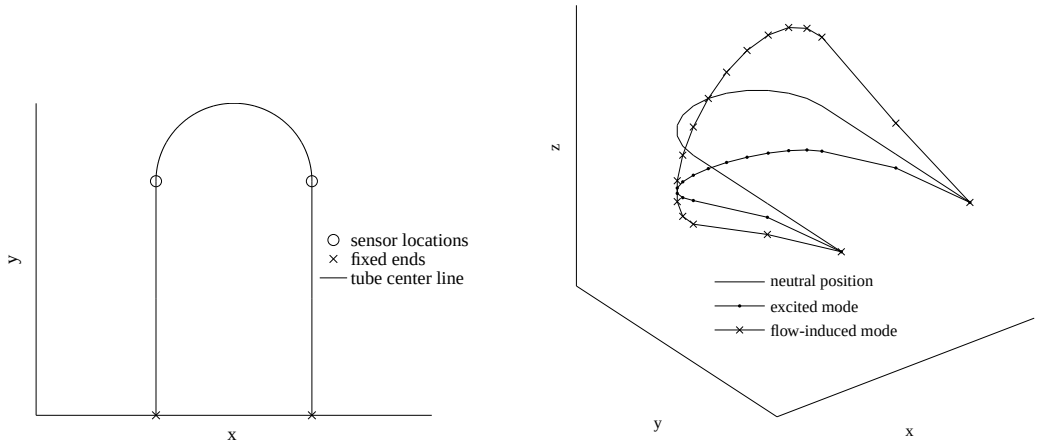

(a) Shape of the tube centerline

(b) Shape of the vibration mode

Figure 1. Typical shape of the tube of a Coriolis mass flow meter

of the fluid. The fluid is considered incompressible and viscous and its inertia properties are modeled as a string moving along the tube centerline. A similar approach was used to model the fluid flow through a beam element in the multibody systems dynamic package SPACAR, which was published previously in Reference [7]. In this paper, those tube elements are used to model the performance of a Coriolis mass flow meter for shape optimization. The tube shape is described by the geometric properties of the cross-section of the elements and the position and orientation of the nodal points. Besides the calculation of the performance criteria for these shape parameters, the model is used to compute the sensitivity (derivatives) of the performance criteria to the shape parameters. The advantage of using the flexible multibody approach over a linear finite element approach is the possibility to consider some deformations as infinitely rigid, which reduces the dimensions of the dynamic equations and speeds up the computations for optimization. Furthermore, the flexible multibody approach as implemented in the package SPACAR already provides some derivatives of kinematic functions to the node locations, which are needed for the computation of the parameter sensitivities. Finally, the described method for computing the parameter sensitivities of the performance criteria can straightforwardly be extended to other systems that can be described by the flexible multibody approach. This approach can describe a wide class of systems including system with infinitely rigid elements, flexible elements and elements undergoing large rotations.

2 PERFORMANCE CRITERIA AND PARAMETERS

A classic shape of the tube of a Coriolis mass flow meter is shown in figure 1(a). The tube is fixed at both ends and the out-of-plane motion of the tube is measured at the two encircled points. The tube is excited in its first eigenmode and a flow induces an additional vibration mode due to the Coriolis-effect. This vibration mode occurs 90 degrees out of phase with the excited mode and results in a phase-difference between the motion of the tube at the sensor locations. The phase-difference is proportional to the mass-flow. Figure 1(b) shows the first eigenmode of the tube without flow and the additional flow induced part of the eigenmode

An extensive discussion on the design of a Coriolis mass flow meter can be found in Reference [5]. An important aspect of the design of a Coriolis mass flow meter is the shape of the tube. The tube shape is specified by the dimensions of the cross-section, e.g., the inner and outer diameter of a circular tube, and the curvature of the tube centerline, e.g., the U-shape. The design of the tube shape affects several quantities related to the performance of a Coriolis mass flow meter. The most important are:

- The measurement sensitivity, which should be large to reduce the effect of sensor noise on the measured mass flow.

- The tube's eigenfrequencies, which should be well separated to reduce the effect of disturbances on the measurement sensitivity.
- The drop of the pressure between the inlet and outlet of the tube, which should be small.
- The envelope of the tube, which should be small.

These issues can be considered as either objective or constraint for the optimization of the tube shape, depending on their relative importance. The last issue is directly related to the tube shape and the other issues depend on the tube shape indirectly. Models are used to quantify those performance criteria for a design of the tube shape. The effect of the tube shape on the pressure drop is modeled using the Hagen–Poiseuille equation, which is not elaborated further in this paper. The paper focuses on modeling the eigenfrequency and the measurement sensitivity.

3 MODELLING

A flexible rigid body model is used to quantify the eigenfrequencies and the measurement sensitivity for a certain choice of the tube shape. The tube shape is specified by two types of shape parameters; the initial location of the nodal points of the elements and parameters related to the cross-section of the element, e.g., the area and the area moment of inertia. The initial nodal locations are denoted by u_i^0 and the cross-sectional parameters are denoted by r_i. These shape parameters and the properties of the fluid and the tube material are used to formulate the kinematic and dynamic equations of the tube elements. The element equations are added and reduced to a minimal set of degrees of freedom to obtain an unconstrained set of global dynamic equations. Eigenfrequency analysis yields the eigenfrequencies and eigenmodes, where the latter are used to compute the measurement sensitivity of the mass flow meter.

This section describes the modeling steps from the element equations to the calculation of the eigenfrequency and the measurement sensitivity. After the derivation of the equations for each of these modeling steps, the computation of the derivative of these equations to the shape parameters is discussed. The derivative of the final model equations gives the sensitivity of the eigenfrequency and the measurement sensitivity to variations of the shape parameters.

3.1 Element kinematics

3.1.1 Model equations

The tube of the mass flow meter is modeled using the tube element that was previously presented in Reference [7]. The tube element is an extension of the two-node beam element described in Reference [4]. The position and orientation of each element are described by the nodal coordinates $\boldsymbol{u} = \left[\boldsymbol{x}^{pT}, \boldsymbol{\lambda}^{pT}, \boldsymbol{x}^{qT}, \boldsymbol{\lambda}^{pT}\right]^T$. Coordinates $\boldsymbol{x}^p$ and $\boldsymbol{x}^q$ are the Cartesian coordinates and coordinates $\boldsymbol{\lambda}^p$ and $\boldsymbol{\lambda}^q$ are the Euler parameters of nodes p and q. In addition to these coordinates, two coordinates related to the mass flow are introduced in Reference [7], but these are not used in this paper, because the mass-flow is assumed to be constant along the tube. The four Euler parameters ($\boldsymbol{\lambda} = [\lambda_0 \dots \lambda_3]^T$) of each node describe the orientation of the orthogonal triad of unit vectors e_{ij} connected to the node. The unit vectors e_{i1}^p and e_{i1}^q are perpendicular to the cross-sections, pointing inwards at node p and outwards at node q. The other unit vectors e_{i2} and e_{i3} are pointing in the principal directions of the cross-section. The norm the four Euler coordinates of each node point is unity and thus the four Euler coordinates define three independent coordinates. So, each element has 12 independent nodal coordinates and six rigid body degrees of freedom. Therefore, six independent deformation functions are defined, which are formulated such that they are invariant for any rigid-body displacement. The following six deformations $\epsilon_1 \dots \epsilon_6$ are defined

$$
\begin{array}{lll}
\epsilon_1 = \bar{\epsilon}_1 + \left(2\bar{\epsilon}_3^2 + \bar{\epsilon}_3\bar{\epsilon}_4 + 2\bar{\epsilon}_4^2 + 2\bar{\epsilon}_5^2 + \bar{\epsilon}_5\bar{\epsilon}_6 + 2\bar{\epsilon}_6^2\right) / \left(30l^0\right), & \bar{\epsilon}_1 = l - l^0, \\
\epsilon_2 = \bar{\epsilon}_2 + \left(-\bar{\epsilon}_3\bar{\epsilon}_6 + \bar{\epsilon}_4\bar{\epsilon}_5\right)/l^0, & \bar{\epsilon}_2 = l^0\left(\boldsymbol{e}_{i3}^p\boldsymbol{e}_{i2}^q - \boldsymbol{e}_{i2}^p\boldsymbol{e}_{i3}^q\right)/2, \\
\epsilon_3 = \bar{\epsilon}_3 + \bar{\epsilon}_2\left(\bar{\epsilon}_5 + \bar{\epsilon}_6\right) / \left(6l^0\right), & \bar{\epsilon}_3 = -l^0\boldsymbol{e}_i^l\boldsymbol{e}_{i3}^p, \\
\epsilon_4 = \bar{\epsilon}_4 - \bar{\epsilon}_2\left(\bar{\epsilon}_5 + \bar{\epsilon}_6\right) / \left(6l^0\right), & \bar{\epsilon}_4 = l^0\boldsymbol{e}_i^l\boldsymbol{e}_{i3}^q, \\
\epsilon_5 = \bar{\epsilon}_5 - \bar{\epsilon}_2\left(\bar{\epsilon}_3 + \bar{\epsilon}_4\right) / \left(6l^0\right), & \bar{\epsilon}_5 = l^0\boldsymbol{e}_i^l\boldsymbol{e}_{i2}^p, \\
\epsilon_6 = \bar{\epsilon}_6 + \bar{\epsilon}_2\left(\bar{\epsilon}_3 + \bar{\epsilon}_4\right) / \left(6l^0\right), & \bar{\epsilon}_6 = -l^0\boldsymbol{e}_i^l\boldsymbol{e}_{i2}^q,
\end{array}
\tag{1}
$$

where the Einstein summation convention is used, $l = \|\boldsymbol{x}^p - \boldsymbol{x}^q\|$ is the actual distance between the nodal points and $\boldsymbol{e}_i^l = (x_i^p - x_i^q)/l$ is the actual unit vector pointing from node p to node q. The initial length l^0 is defined such that $\epsilon_1 = 0$ for the initial nodal coordinates u_i^0. These functions, relating the deformations to the nodal coordinates, are denoted as $\epsilon_i = \mathcal{D}_i(\boldsymbol{u})$. For kinematic analysis, the first and second order derivatives of the expressions for $\mathcal{D}_i(\boldsymbol{u})$ with respect to u_i, denoted as $\frac{\partial}{\partial u_j}\mathcal{D}_i$ and $\frac{\partial^2}{\partial u_j \partial u_k}\mathcal{D}_i$, are used. These (lengthy) expressions, which can be found in [4], are not elaborated further in this paper.

3.1.2 Sensitivities

The kinematic functions $\mathcal{D}_i(\boldsymbol{u})$ do not depend on the cross-section parameters and thus the derivatives of the kinematic functions to these shape parameters are zero.

The derivatives of the kinematic functions to the initial nodal coordinates can be computed using the derivatives of the kinematic functions to the actual nodal coordinates, but these derivatives are not the same, because the undeformed length l^0 depends on the initial nodal coordinates, but not on the actual nodal coordinates. Thus, the derivatives of the kinematic functions to the initial nodal coordinates can be computed from

$$\frac{\partial}{\partial u_j^0}\mathcal{D}_i = \frac{\partial}{\partial u_j}\mathcal{D}_i + \frac{\partial}{\partial l^0}\mathcal{D}_i \frac{\partial}{\partial u_j^0} l^0, \tag{2}$$

where the relations for $\frac{\partial}{\partial u_j}\mathcal{D}_i$ are described in [4], $\frac{\partial}{\partial l^0}\mathcal{D}_i$ is obtained from the relations for $\boldsymbol{\epsilon}$ and $\boldsymbol{epsilon}$ and $\frac{\partial}{\partial u_j^0} l^0$ is obtained from the condition $\epsilon_1 = 0$ for u_i^0, which results in a linear relation in l^0.

3.2 Element dynamics

3.2.1 Model equations

The energetic duals of the nodal coordinates u_i are the nodal forces f_i, such that $f_i \delta u_i$ represents the virtual work exerted by those forces, where the prefix δ denotes a virtual variation. Similarly, the energetic duals of the deformations ϵ_i are the generalized stresses σ_i, where $-\sigma_i \delta \epsilon_i$ represents the virtual work exerted by those stresses. The equilibrium conditions for each element is formulated as

$$\delta u_i \left(M_{ij}\ddot{u}_j - f_i\right) - \delta\epsilon_i \sigma_i = 0, \tag{3}$$

where M_{ij} is the mass matrix and f_i includes the inertial terms that are not depending on the acceleration of the nodal coordinates, like Coriolis forces. Hereafter, expressions for the nodal forces, the mass matrix and the internal stresses for the tube element are described shortly. Those expressions were previously published in Reference [7] and are an extension of the model for two-node beam element described in References [6, 4].

The generalized stresses in the flexible tube elements are modeled by the following constitutive relations for stretching, bending and torsion

$$\sigma_i = K_{ij}\left(\epsilon_j - \epsilon_j^0\right), \tag{4}$$

where ϵ_j^0 is the value of the deformation ϵ_j for which the beam is stress free and the nonzero elements of stiffness matrix K_{ij} are

$$\begin{aligned} K_{11} &= l^0/E/A, & K_{22} &= Gk_xI_t/l^{03}, & K_{33} &= K_{44} = 4EI_y/l^{03}, \\ K_{34} &= K_{43} = -2EI_y/l^{03}, & K_{55} &= K_{66} = 4EI_z/l^{03}, & K_{56} &= K_{65} = -2EI_z/l^{03}, \end{aligned} \tag{5}$$

E is the modulus of elasticity of the tube material, G is its shear modulus, A is the area of the tube's cross-section, I_y, I_z are the moments of inertia of the tube's cross-section around the local y- and z-axis, I_t is the torsion consant and k_x is a shape factor, which is 1 for circular cross-sections. The effect of traverse shear and the internal pressure on the internal stresses are expected to be small and thus not taken into account in the constitutive relations.

The mass matrix M_{ij} and the inertia force vector f_i that result from the inertia of the tube and the flow are

$$M_{ij} = \left(\rho A + \tilde{\rho}\tilde{A}\right) l^0 \frac{\partial}{\partial u_i}\mu_k \Phi_{kl} \frac{\partial}{\partial u_j}\mu_l + 2\rho I_p l^0 L_{ki} L_{kj}, \tag{6}$$

$$f_i = -\left(\rho A + \tilde{\rho}\tilde{A}\right) l^0 \frac{\partial}{\partial u_i}\mu_k \Phi_{kl} \frac{\partial^2}{\partial u_m \partial u_n}\mu_l \dot{u}_m \dot{u}_n - 4\rho I_p l^0 \dot{L}_{ki} L_{km} \dot{u}_m \tag{7}$$

$$2\tilde{\rho}\tilde{v}\tilde{A}\frac{\partial}{\partial u_i}\mu_k \Phi'_{kl} \frac{\partial}{\partial u_j}\mu_l \dot{u}_j - 2\tilde{\rho}\tilde{v}^2 \tilde{A}\tilde{k}/l^0 \frac{\partial}{\partial u_i}\mu_k \Phi''_{kl}\mu_l, \tag{8}$$

where ρ is the density of the tube material, I_p is the polar moment of inertia, $\tilde{\rho}$ is the density of the fluid, $\tilde{A}$ is the area of the tube's cross-section containing fluid, $\tilde{k}$ is a factor that measures the deviation from a uniform velocity distribution (1 for a uniform flow distribution and 4/3 for a laminar flow through a circular cross-section), and furthermore

$$\mathbf{\Phi} = \frac{1}{420}\begin{bmatrix} 156I_3 & 22I_3 & 54I_3 & -13I_3 \\ 22I_3 & 4I_3 & 13I_3 & -3I_3 \\ 54I_3 & 13I_3 & 156I_3 & -22I_3 \\ -13I_3 & -3I_3 & -22I_3 & 4I_3 \end{bmatrix}, \mathbf{\Phi}' = \frac{1}{60}\begin{bmatrix} -30I_3 & 6I_3 & 30I_3 & -6I_3 \\ -6I_3 & O_3 & 6I_3 & -I_3 \\ -30I_3 & -6I_3 & 30I_3 & 6I_3 \\ 6I_3 & I_3 & -6I_3 & O_3 \end{bmatrix}, \mathbf{\Phi}'' = \frac{1}{30}\begin{bmatrix} -36I_3 & -33I_3 & 36I_3 & -3I_3 \\ -3I_3 & -4I_3 & 3I_3 & I_3 \\ 36I_3 & 3I_3 & -36I_3 & 33I_3 \\ -3I_3 & I_3 & 3I_3 & -4I_3 \end{bmatrix}.$$

$$\mu_{\{1\ldots3\}} = x_i^p, \mu_{\{4\ldots6\}} = l^0 e_{i1}^p,\ \mu_{\{7\ldots9\}} = x_i^q,\ \mu_{\{10\ldots12\}} = l^0 e_{i1}^q, \tag{9}$$

$$L_{\{1\ 4\ldots7\}} = \{-\lambda_1^p, \lambda_0^p, \lambda_3^p, -\lambda_2^p, \},\ L_{\{2\ 11\ldots14\}} = \{-\lambda_1^q, \lambda_0^q, \lambda_3^q, -\lambda_2^q, \}, \tag{10}$$

The first term in the mass matrix and force vector account for the mass of the tube and the fluid, which are assumed to be distributed along the element's centerline. The second term in the mass matrix and force vector account for the moment of inertia of the tube material around the element's centerline, which is lumped at the nodal points. The third term in the force vector is due to the Coriolis acceleration of the fluid. The fourth term in the force vector is due to the centripetal acceleration of the flow in the curved sections.

3.2.2 Sensitivities

The derivatives of K_{ij}, M_{ij} and f_i to the cross-sectional parameters $(A, I_x, I_y, I_p, I_t, k_x, \tilde{A}, \tilde{k})$ can be obtained by straightforward differentiation of (5), (6) and (8).

The stiffness matrix K_{ij} only depends on the initial nodal coordinates via the initial length l^0. Thus, $\frac{\partial}{\partial u_m^0}K_{ij}$ can be computed from the chain rule for differentiation using $\frac{\partial}{\partial l^0}K_{ij}\frac{\partial}{\partial u_m^0}l^0$ that can be computed straightforwardly from (5) and $\frac{\partial}{\partial u_m^0}l^0$ that was previously used for the kinematic computations.

The mass matrix M_{ij} and the inertia force vector f_i depend on the nodal coordinates via l^0, L_{ij}, μ_i and derivatives of μ_i. The derivatives $\frac{\partial}{\partial u_m^0}l^0$ were previously used for the kinematic computations. L_{ij} is linear in the nodal Euler parameters and its derivative to the nodal coordinates can thus be computed straightforwardly. The derivatives of μ_i to the nodal coordinates can be obtained from the derivatives of l^0, which were previously used, the derivatives of x_i^p and x_i^q, which are unity for the respective nodal coordinates, and the derivatives of e_{i1}^p and e_{i1}^q, which can be computed from the expression for rotation of these vectors, which are quadratic in the Euler parameters

3.3 Equations of motion

3.3.1 Model equations

The equations of motion are formulated in terms of a set of independent coordinates q_i, which are referred to as the degrees of freedom (DOFs). Given the fixed nodal coordinates and rigid deformations of the system, which are both prescribed zero, those independent coordinate are a subset of u_i and ϵ_i that are exactly sufficient to define all other u_i and ϵ_i via the kinematic relations $\mathcal{D}_i(\boldsymbol{u})$. In the considered problem, the deformations 2...6 of all elements, except for the last element, are used as degree of freedom. The first deformation mode is not taken into account, because the elements are considered stiff in the elongation direction, and the corresponding first deformation is prescribed zero. The six deformations of the last element can be computed from the deformations of the other elements, because the elements form a loop

with fixed ends, and thus these deformations are not included in the set of DOFs. The relations between all coordinates and the DOFs are expressed by,

$$u_i = \mathcal{F}_i^{(u)}(q_i),\ \epsilon_i = \mathcal{F}_i^{(\epsilon)}(q_i), \tag{11}$$

where $\mathcal{F}_i^{(u)}$ and $\mathcal{F}_i^{(\epsilon)}$ are geometric transfer functions. The first and second order derivatives of those transfer functions with respect to q_i, expressed by $\frac{\partial}{\partial q_j}\mathcal{F}_i$ and $\frac{\partial^2}{\partial q_j \partial q_k}\mathcal{F}_i$, are computed from the derivatives of $\mathcal{D}_i\left(\boldsymbol{u}\right)$ with respect to u_i as derived in Reference [3] and implemented in the multibody systems dynamic package SPACAR. These (lengthy) expressions are not elaborated here.

Using the derivatives of the geometric transfer functions and the principle of virtual power (see Reference [3]), the dynamic equations of the system can be expressed in terms of the DOFs as

$$\frac{\partial}{\partial q_i}\mathcal{F}_k^{(x)} M_{kl}^{(x)} \frac{\partial}{\partial q_j}\mathcal{F}_l^{(x)} \ddot{q}_j = \frac{\partial}{\partial q_i}\mathcal{F}_k^{(x)} \left(f_k^{(x)} - M_{kl}^{(x)} \frac{\partial^2}{\partial q_m \partial q_j}\mathcal{F}_l^{(x)} \dot{q}_m \dot{q}_j \right) - \frac{\partial}{\partial q_i}\mathcal{F}_k^{(\epsilon)} \sigma_k^{(\epsilon)}, \tag{12}$$

where $M_{ij}^{(x)}$ is the global mass matrix, $f_j^{(x)}$ is the global force vector, including inertia forces, and $\sigma_j^{(\epsilon)}$ is the global stress vector. The global mass matrix, force vector and stress vector are obtained by assembling those of the individual elements. Assembly of the constitutive element equations ((4)) results in the global stiffness matrix $K_{ij}^{(\epsilon)}$ that relates the global stress vector to the global deformation vector.

In the considered problem, small vibrational motions with respect to a static nominal configuration are considered. For frequency analysis, the equations of motion are linearized using the method described in [2]. The resulting linearized relations contain dynamic and geometric stiffening matrices with elements proportional to the square of the fluid velocity. Because only small flows are considered, these matrices are small and neglected in further analysis. The remaining linear equations of motion are

$$M_{ij}^{(q)} \delta\ddot{q}_j + C_{ij}^{(q)} \delta\dot{q}_j + K_{ij}^{(q)} \delta q_j = O_i, \tag{13}$$

where $M_{ij}^{(q)}$ is the mass matrix, $C_{ij}^{(q)}$ the velocity sensitive matrix and $K_{ij}^{(q)}$ is the structural stiffness matrix. These matrices are obtained from

$$M_{ij}^{(q)} = \frac{\partial}{\partial q_i}\mathcal{F}_k^{(x)} M_{kl}^{(x)} \frac{\partial}{\partial q_j}\mathcal{F}_l^{(x)},\ C_{ij}^{(q)} = \frac{\partial}{\partial q_i}\mathcal{F}_k^{(x)} \frac{\partial}{\partial \dot{u}_l} f_k \frac{\partial}{\partial q_j}\mathcal{F}_l^{(x)},\ K_{ij}^{(q)} = \frac{\partial}{\partial q_i}\mathcal{F}_k^{(\epsilon)} K_{kl}^{(\epsilon)} \frac{\partial}{\partial q_j}\mathcal{F}_l^{(\epsilon)}. \tag{14}$$

The mass and stiffness matrix are symmetric. The velocity sensitive matrix is skew symmetric and its elements are linear in the flow velocity $\tilde{v}$.

3.3.2 Sensitivity

The sensitivity of the dynamic matrices to the shape parameters p_n can be computed straightforwardly from the product rule for differentiation using the parameter derivatives of the dynamic matrices $\frac{\partial}{\partial p_n}M_{kl}^{(x)}$, $\frac{\partial^2}{\partial q_l \partial p_n} f_k$ and $\frac{\partial}{\partial p_n}K_{kl}^{(\epsilon)}$, which are obtained from assembling the derivatives of the element matrices, and the derivatives of the geometric transfer functions $\frac{\partial^2}{\partial q_i \partial p_n}\mathcal{F}_k^{(x)}$ and $\frac{\partial^2}{\partial q_i \partial p_n}\mathcal{F}_k^{(\epsilon)}$. The derivatives of the geometric transfer functions do not depend on the cross-sectional parameters and thus $\frac{\partial^2}{\partial q_i \partial r_j}\mathcal{F}_k^{(\epsilon)} = O_{kij}$, which simplifies the computations of the derivatives of the dynamic matrices to the cross-sectional parameters. The derivatives of $\frac{\partial}{\partial q_i}\mathcal{F}_k^{(x)}$ to the nodal coordinates are derived from the expressions to compute $\frac{\partial}{\partial q_i}\mathcal{F}_k^{(x)}$ from $\frac{\partial}{\partial q_i}\mathcal{D}_i$ and the previously described expressions for the derivatives of $\frac{\partial}{\partial q_i}\mathcal{D}_i$ to the nodal coordinates. The expression are not elaborated further in this paper.

3.4 Eigenfrequencies and eigenmodes

3.4.1 Model equations

The eigenvalue and eigenvector of the dynamic equations (13) are the solutions of

$$\left(\omega^2 M_{ij}^{(q)} + \omega C_{ij}^{(q)} + K_{ij}^{(q)}\right) v_j^{(q)} = O_i, \tag{15}$$

where only the solution for the lowest eigenvalue ω is considered. The eigenvector $v_j^{(q)}$ denotes the first resonance vibration mode of the system in terms of the DOFs, which is scaled such that

$$v_i^{(q)} M_{ij}^{(q)} v_j^{(q)} = 1. \tag{16}$$

Without fluid flow ($\tilde{v} = 0$), the velocity sensitive matrix $C_{ij}^{(q)}$ is zero and the eigenmode is real. For nonzero fluid flow, $C_{ij}^{(q)}$ is nonzero and the eigenmode becomes complex, which means that the degrees of freedom do not vibrate in the same phase. The mass flow is measured from the phase-difference of the vibration mode at the two node points corresponding to the sensor locations. The vibration mode $v_i^{(q)}$, which is expressed in terms of the the DOFs q, is converted to the vibration mode in terms of the nodal coordinates u by the following transformation

$$v_j^{(x)} = \frac{\partial}{\partial q_i} \mathcal{F}_j^{(x)} v_i^{(q)}. \tag{17}$$

3.4.2 Sensitivity

The parameter derivatives of the eigenvalue and eigenvector in terms of the DOFs are computed using the method described in Reference [1], which is suited for non-proportionally damped systems. This method computes the parameter derivatives of the eigenvalue and eigenvector from the solution of the eigenvalue problem, the dynamic matrices $M_{ij}^{(q)}$, $C_{ij}^{(q)}$ and $K_{ij}^{(q)}$ and the parameter derivatives of these dynamic matrices. The scaling of the eigenvalues in (16) differs from the scaling used in Reference [1] and therefore the method has been modified slightly.

The parameter sensitivity of the vibration mode in terms of the nodal coordinates can be computed from differentiation of (17) using the previously derived parameter derivative of the vibration mode in terms of the DOFs and the parameter derivative of $\frac{\partial}{\partial q_i} \mathcal{F}_k^{(\epsilon)}$, which was previously used for the computation of the parameter derivatives of the dynamic matrices.

3.5 Measurement Sensitivity

3.5.1 Model equations

The mass flow is measured from the phase-difference of the vibration mode of the tube at two sensor locations. This phase difference is obtained from the model by subtracting the complex angles of the components of the eigenmode $v_j^{(x)}$ corresponding to the nodes at the sensor locations. The complex angles are assumed to be small, such that the phase difference between the nodal points n and m can be approximated by

$$\theta_{nm} = \frac{\mathcal{I}\left(v_n^{(x)}\right)}{\mathcal{R}\left(v_n^{(x)}\right)} - \frac{\mathcal{I}\left(v_m^{(x)}\right)}{\mathcal{R}\left(v_m^{(x)}\right)}. \tag{18}$$

The phase difference θ_{nm} is proportional to the mass flow $\tilde{v}$. The measurement sensitivity z is the phase difference per unit mass flow, which can be computed from

$$z = \frac{\theta_{nm}}{\tilde{A}\tilde{\rho}\tilde{v}}. \tag{19}$$

3.5.2 Sensitivity

The sensitivity of the phase difference θ_{nm} to parameter p_o can be computed from differentiation of (18), resulting in

$$\frac{\partial}{\partial p_o}\theta_{nm} = \frac{\mathcal{I}\left(\frac{\partial}{\partial p_o} v_n^{(x)}\right)}{\mathcal{R}\left(v_n^{(x)}\right)} - \frac{\mathcal{I}\left(v_n^{(x)}\right)}{\mathcal{R}\left(v_n^{(x)}\right)^2}\mathcal{R}\left(\frac{\partial}{\partial p_o} v_n^{(x)}\right) - \frac{\mathcal{I}\left(\frac{\partial}{\partial p_o} v_m^{(x)}\right)}{\mathcal{R}\left(v_m^{(x)}\right)} + \frac{\mathcal{I}\left(v_m^{(x)}\right)}{\mathcal{R}\left(v_m^{(x)}\right)^2}\mathcal{R}\left(\frac{\partial}{\partial p_o} v_m^{(x)}\right), \tag{20}$$

where the derivation of $\frac{\partial}{\partial p_n} v_n^{(x)}$ has been discussed before.

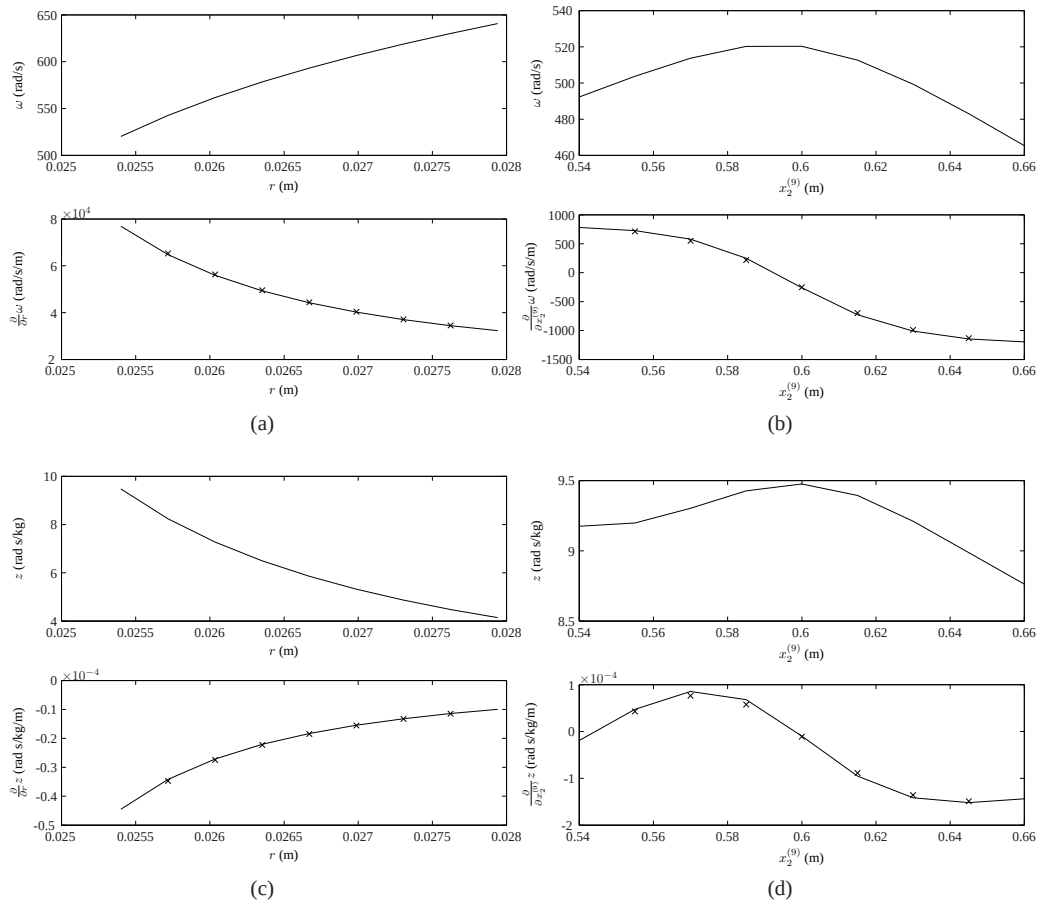

Figure 2. Results from sensitivity analysis

Finally, the parameter sensitivity of z can be computed from differentiation of (19) using the previously derived expression for $\frac{\partial}{\partial p_o}\theta_{nm}$.

4 RESULTS

4.1 Modelling

The model is verified by computing the eigenfrequency and sensitivity of the U-shaped mass flow meter described in Reference [8] and comparing the results to References [8] and [7]. The U-shaped tube is depicted in Figure 1(a). The tube is made of steel with E = 208 GPa, G = 80 GPa and ρ = 8027 kg/m^3. The fluid is water with $\tilde{\rho}$ = 1000 kg/m^3. A radius of a =150 mm is taken for the semicircular part and the length of the straight sections is set to b =450 mm. The cross-section of the tube is circular with an outer diameter r of 50.8 mm and an inner diameter of 47.2 mm. The two straight sections are subdivided into two elements and the semicircular part is subdivided into 12 pre-curved elements.

The model presented in the previous section yields an eigenfrequency of $\omega = 520$ rad/s and a sensitivity of $z = 9.48{\cdot}10^{-4}$ rad s/kg, which can also be rewritten as $\omega = 0.177\sqrt{EI(\rho A + \tilde{\rho}\tilde{A})}/a^2$ and $z = 1.82{\cdot}10^{-6}\omega$ s^2/kg. These values are the same as those found in Reference [7] for low flows.

4.2 Sensitivity

The proposed method to compute the parameter sensitivities is verified by computing some of the parameter sensitivities for the U-shaped tube and comparing them to the parameter derivatives obtained from

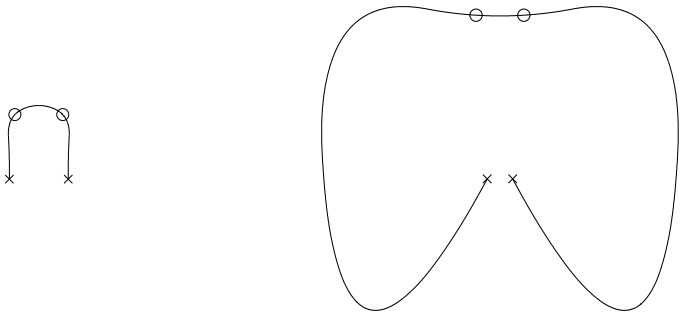

(a) Initial shape (b) Final shape

Figure 3. Results from optimization

numerical differences. The parameter sensitivities of the eigenfrequency and the measurement sensitivity are computed. The sensitivities are computed for the outer radius of the tube, which is a cross-sectional parameter affecting both the inertia and stiffness of the tube material. Moreover, the sensitivities are computed for the nodal point at the centerline of the U, which is moved in the y-direction. The orientation of the tube at the nodal points is kept constant. Figure 2 shows the result of the sensitivity calculations. The outer radius is varied over 9 values between the original radius and a 10% larger radius. The nodal point is varied over 9 values between 90% and 110% of the original distance from the fixed ends. The figures show the variation of the performance criteria and the sensitivity of those criteria to the shape parameters. Moreover, an approximate derivative, indicated by crosses, is computed from the division of difference between the next and the previous value of the performance criterion and the difference between the next and previous value of the shape parameter. Note that the sensitivities match the approximate derivatives closely, the difference reduces even more if the grid for computing the approximate derivatives is refined.

4.3 Optimization

The developed model was used for the actual optimization of the tube shape of a Coriolis mass flow meter. Details on the optimization are published in Reference [9]. Figure 3 shows the initial U-shaped tube and the optimized tube shape. The sensitivity of the final shape is 68 times the sensitivity of the initial shape. Most of this improvement is the result of the increased length of the tube, which could not be increased further due to constraints on the envelope and the allowed drop of pressure along the tube. A small part of the improvement results from the change of the shape.

The parameter sensitivities of the performance criteria were not used for obtaining the presented results. Future optimizations might benefit from the availability of these parameter sensitivities. The sensitivities have already been used to verify the robustness of the obtained design and to analyze the effect of the cross-sectional parameters on the various constraints.

5 CONCLUSIONS

Modeling a Coriolis mass flow meter for shape optimization is considered in this paper. The model-based optimization should enhance the performance of a Coriolis mass flow sensor by optimizing the shape of the tube. Typical performance criteria for the optimization are the measurement sensitivity and the separation of the eigenfrequencies. The tube shape is specified by the dimensions of the cross-section and the curvature of the tube centerline.

The dynamics of the meter's tube are modeled using a flexible multibody approach. An existing beam

element is extended to model the distributed flexibility and inertia of the fluid-conveying tube. The element equations are assembled, reduced to a minimal set of degrees of freedom and linearized. Modal analysis of the linearized dynamic equations yields the eigenfrequency and measurement sensitivity of the tube.

The model is also used to derive the parameter sensitivities of the performance criteria to the shape parameters. The dynamic equations of the model are differentiated to the shape parameters and the method presented in Reference [1] is used to derive the parameter sensitivities of the eigenvalue and measurement sensitivity. The parameter sensitivities are useful for the shape optimization and they can also be used to analyze the sensitivity and the robustness of the performance criteria to changes of the shape parameters.

The advantage of using the flexible multibody approach over a conventional linear finite element approach is the possibility to consider some deformations as infinitely rigid, which reduces the dimensions of the dynamic equations and speeds up the computations for optimization. Furthermore, the flexible multibody approach implemented in the package SPACAR provides derivatives of the element deformations to nodal coordinates which are used for the sensitivity analysis.

The model is validated by comparison of the resulting eigenfrequency and measurement sensitivity to the results for a U-shaped Coriolis mass flow meter from Reference [8]. The U-shaped mass flow meter is also used to validate the parameter sensitivities by comparison to the values obtained from finite differences. Furthermore, preliminary results from the optimization of the tube shape using the presented model are presented. So far, the parameter sensitivities have not been used for optimization. Future research will show the usability of the parameter sensitives for the optimization.

The proposed method for computing the parameter sensitivities of dynamic properties can straightforwardly be extended to other systems that can be described by the flexible multibody approach. This approach can describe a wide class of systems including system with infinitely rigid elements, flexible elements and elements undergoing large rotations. Application of the proposed method to the optimization of to other (multibody) systems will be subject of future research.

REFERENCES

[1] FRISWELL, M., AND ADHIKARI, S. Derivatives of complex eigenvectors using nelson's method. *AIAA Journal 38* (2000), 2355–2357.

[2] JONKER, J., AARTS, R., AND VAN DIJK, J. A linearized input-output representation of flexible multibody systems for control synthesis. *Multibody System Dynamics 21* (2009), 99–122.

[3] JONKER, J., AND MEIJAARD, J. *Multibody Systems Handbook*. Springer-Verlag, Heidelberg, 1990, ch. SPACAR - computer program for dynamic analysis of flexible spatial mechanisms and manipulators, pp. 123–143.

[4] JONKER, J., AND MEIJAARD, J. Definition of deformation parameters for beam elements and their use in flexible multibody system analysis. In *Proceedings of the ECCOMAS Thematic Conference* (Warsaw, Poland, June-July 2009), K. Arczewski, J. Fraczek, and M. Wojityra, Eds., pp. 1–20.

[5] MEHENDALE, A. *Coriolis Mass Flow Rate Meters for Low Flows*. PhD thesis, University of Twente, October 2008.

[6] MEIJAARD, J. Validation of flexible beam elements in dynamic programs. *Nonlinear Dynamics 9* (1996), 21–36.

[7] MEIJAARD, J., AND HAKVOORT, W. Modelling of fluid-conveying flexible pipes in multibody systems. In *Proceedings of the 7th EUROMECH Solid Mechanics Conference* (Lisbon, Portuga, 7-11 September 2009), J. A. et.al., Ed.

[8] SULTAN, G., AND HEMP, J. Modelling of the coriolis mass flowmeter. *Journal of Sound and Vibration 132*, 2 (1989), 473–489.

[9] TIN, L. D. Towards optimization of micro-coriolis flow sensors. In *Posters at the MicroNano Conference* (Delft, The Netherlands, November 2009).